Available online at www.sciencedirect.com
ScienceDirect
Journal of Sound and Vibration 318 (2008) 982–990
JOURNAL OF SOUND AND VIBRATION
www.elsevier.com/locate/jsvi

Exact two-dimensional solutions for in-plane natural frequencies of laminated circular arches

Q. Lü, C.F. Lü*

Department of Civil Engineering, Zhejiang University, Zheda Road, No. 38, Hangzhou 310027, PR China

Received 26 September 2007; received in revised form 3 May 2008; accepted 10 May 2008
Handling Editor: L.G. Tham
Available online 17 June 2008

Abstract

Exact analysis on the in-plane free vibration of simply supported laminated circular arches is carried out based on the two-dimensional theory of elasticity. The method of separation of variables is employed to expand all the variables into Fourier series about the longitudinal coordinate, so that the system of partial differential equations is reduced to the ordinary one about the radial coordinate. The state space method is used to derive a series of simultaneous first-order differential equations. Due to the variable coefficients posed by the radial coordinate, analytical solutions are rather unpractical, and hence the approximate laminate model is adopted to translate the state equation into the one with constant coefficients. The relation between the state vector at the inner and outer surface of the arch is finally obtained according to the continuity conditions at interfaces and the traction free conditions at the two lateral surfaces. The formulation is validated by comparing the present results to those available in literature. Effects of geometric parameters and stacking sequences on the natural frequencies of circular arches are investigated and discussed. Numerical results presented in this paper provide benchmarks for future analysis of circular arches.

1. Introduction

Planar curved beams including circular arches are one of the most predominant components in engineering structures, such as bridges, turbo-machinery blades, aircraft structures, and so on. Natural frequencies are the basic and substantial issue for the design and use of such structural components, due to which free vibration of curved beams has been attracting intensive researches during the past few decades. Free vibration of homogeneous isotropic curved beams were widely reported and well reviewed in Refs. [1–7], while that for the orthotropic laminated composite counterparts can be found in Refs. [8–13]. It is established however that the application of classical arch theory (CAT) is highly confined to slender geometry due to the Kirchhoff hypothesis where the shear deformation and rotary inertia are neglected [4]. As a result, the deflection is always under-estimated while the natural frequencies and buckling loads are over-predicted. Although the first-order arch theories (FOATs) account for such effects [11,12] by regarding the shear deformation as

*Corresponding author. Tel.: +86 571 8795 2284; fax: +86 571 8795 2165.
E-mail address: lucf@zju.edu.cn (C.F. Lü).

0022-460X/$ - see front matter © 2008 Elsevier Ltd. All rights reserved.
doi:10.1016/j.jsv.2008.05.011

constant through the thickness direction, the accuracy of results are highly dependent on the choice of shear correction factor and the determination of the latter is a rather cumbersome task. In addition, the FOATs are only applicable to thin and moderately thick laminates but not to strongly thick arches and that with highly flexible materials. For strongly thick laminates, Khdeir and Reddy [10] proposed a uniform higher-order arch theory (HOAT) which can be reduced to CAT, FOAT and second-order arch theory (SOAT) with proper definition of deformation parameters, while Matsunaga [13] developed a global HOAT in which both in-plane displacement components are expanded into an infinite series of the thickness-wise coordinate. These HOATs can practically yield more accurate results than the CAT, FOATs and SOATs, but it looks rather difficult to interpret physically the terms related to the higher order of the thickness-wise coordinate.

In this paper, an exact solution, based on the two-dimensional (2D) theory of elasticity, is developed for the in-plane free vibration of circular arches. The arches are assumed simply supported at two ends, for which all variables are expanded into Fourier series about the longitudinal coordinate. Based on the concept of state space method [14], the system of partial differential equations is then reduced into an ordinary differential state equation about the radial coordinate with variable coefficients. For this equation, the approximate laminate model is employed to translate it into the one with constant coefficients. A unique solution is finally obtained for the extremely thin artificial layer. The formulations are validated by comparing numerical results to those available in literature for isotropic and laminated arches. Effects of geometric and material properties on natural frequencies of laminated composite and functionally graded arches are finally discussed.

2. Basic equations and state space formulations

Consider an m-layered laminated circular arch with a total thickness of H, and each layer having the thickness of h_k, as depicted in Fig. 1. The subtended angle is θ_0, the radius of the mid-surface of the arch is R_0, and thus the length of the centerline AA' is $L_0 = \theta_0 R_0$. The Cartesian coordinate system r–θ is established so that $R_0 - \frac{1}{2}H \leqslant r \leqslant R_0 + \frac{1}{2}H$, and $0 \leqslant \theta \leqslant \theta_0$.

If introducing a new coordinate axis $z = r - R_0$, which is originated from and perpendicular to the centerline of the arch and has the same positive direction as the r-axis (see Fig. 1), the basic equations of the arch of orthotropic materials are expresses as

The kinematics equations:

$$\varepsilon_\theta = \frac{1}{R_0 + z}\frac{\partial u_\theta}{\partial \theta} + \frac{u_r}{R_0 + z},\ \varepsilon_r = \frac{\partial u_r}{\partial z},\ \gamma_{\theta r} = \frac{\partial u_\theta}{\partial z} - \frac{u_\theta}{R_0 + z} + \frac{1}{R_0 + z}\frac{\partial u_r}{\partial \theta}. \tag{1}$$

The constitutive equations:

$$\sigma_\theta = C_{11}\varepsilon_\theta + C_{13}\varepsilon_r, \quad \sigma_r = C_{13}\varepsilon_\theta + C_{33}\varepsilon_r, \quad \tau_{\theta r} = C_{55}\gamma_{\theta r}, \tag{2}$$

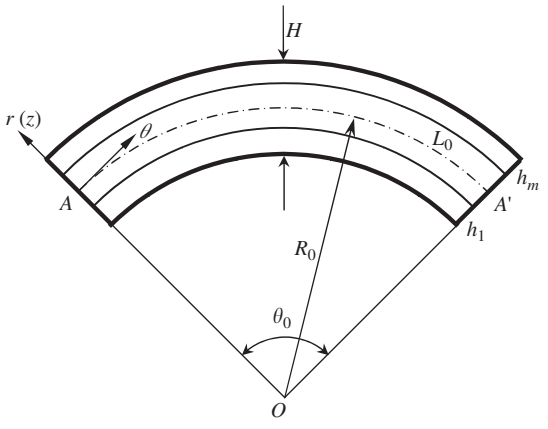

Fig. 1. Geometry and coordinate system of a circular arch.

where C_{ij} are the reduced stiffness constants of orthotropic laminated materials determined by the engineering constants [15].

The equations of motion:

$$\frac{1}{R_0+z}\frac{\partial\sigma_\theta}{\partial\theta}+\frac{\partial\tau_{\theta r}}{\partial z}+\frac{2\tau_{\theta r}}{R_0+z}=\rho\frac{\partial^2 u_\theta}{\partial t^2},\quad \frac{1}{R_0+z}\frac{\partial\tau_{\theta r}}{\partial\theta}+\frac{\partial\sigma_r}{\partial z}+\frac{\sigma_r-\sigma_\theta}{R_0+z}=\rho\frac{\partial^2 u_r}{\partial t^2}. \tag{3}$$

Following the routine job of state space method [14], the above system of equations can be reduced to the following simultaneous first-order differential equations about z:

$$\begin{aligned}
\frac{\partial u_\theta}{\partial z}&=\frac{u_\theta}{R_0+z}-\frac{1}{R_0+z}\frac{\partial u_r}{\partial\theta}+\frac{1}{C_{55}}\tau_{\theta r},\\
\frac{\partial u_r}{\partial z}&=-\frac{C_{13}}{C_{33}}\frac{1}{R_0+z}\frac{\partial u_\theta}{\partial\theta}-\frac{C_{13}}{C_{33}}\frac{1}{R_0+z}u_r+\frac{1}{C_{33}}\sigma_r,\\
\frac{\partial\sigma_r}{\partial z}&=\frac{D}{(R_0+z)^2}\left(\frac{\partial u_\theta}{\partial\theta}+u_r\right)+\rho\frac{\partial^2 u_r}{\partial t^2}+\frac{1}{R_0+z}\left(\frac{C_{13}}{C_{33}}-1\right)\sigma_r-\frac{1}{R_0+z}\frac{\partial\tau_{\theta r}}{\partial\theta},\\
\frac{\partial\tau_{\theta r}}{\partial z}&=\rho\frac{\partial^2 u_\theta}{\partial t^2}-\frac{D}{(R_0+z)^2}\left(\frac{\partial^2 u_\theta}{\partial\theta^2}+\frac{\partial u_r}{\partial\theta}\right)-\frac{C_{13}}{C_{33}}\frac{1}{R_0+z}\frac{\partial\sigma_r}{\partial\theta}-\frac{2}{R_0+z}\tau_{\theta r},
\end{aligned} \tag{4}$$

where $D=C_{11}-C_{13}^2/C_{33}$. Eq. (4) is the well-known state equation, where u_θ, u_r, σ_r, $\tau_{\theta r}$ are termed as the state variables, accompanied with which the induced variable is obtained as

$$\sigma_\theta=\frac{D}{R_0+z}\left(\frac{\partial u_\theta}{\partial\theta}+u_r\right)+\frac{C_{13}}{C_{33}}\sigma_r. \tag{5}$$

For the arch with both ends simply supported, we assume

$$\begin{Bmatrix} u_\theta\\ u_r\\ \sigma_r\\ \tau_{\theta r}\end{Bmatrix}=\sum_{n=1}^{\infty}\begin{Bmatrix} HU(\zeta)\cos(n\pi\xi)\\ HW(\zeta)\sin(n\pi\xi)\\ C_{550}Y(\zeta)\sin(n\pi\xi)\\ C_{550}\Gamma(\zeta)\cos(n\pi\xi)\end{Bmatrix}e^{i\omega t}, \tag{6}$$

where $\zeta=z/H$, $\xi=\theta/\theta_0$, n is the half-wave number along the θ-axis, ω the circular frequency, C_{550} the elastic constant at the inner surface of the arch, t the time coordinate, and $i=\sqrt{-1}$ the imaginary unit. With the introduction of Eq. (6), the partial differential equations in Eq. (4) are reduced to the following non-dimensional state equation of ordinary differential form:

$$\frac{d}{d\zeta}\boldsymbol{\delta}(\zeta)=\mathbf{M}(\Omega,\zeta)\boldsymbol{\delta}(\zeta), \tag{7}$$

where $\boldsymbol{\delta}=\begin{bmatrix} U & W & Y & \Gamma\end{bmatrix}^{\mathrm{T}}$ is called the state vector, and the coefficient matrix is

$$\mathbf{M}=\begin{bmatrix}
\frac{\kappa_r}{\eta} & -\frac{k_n}{\eta} & 0 & \frac{C_{550}}{C_{55}}\\
\frac{C_{13}k_n}{C_{33}\eta} & -\frac{C_{13}\kappa_r}{C_{33}\eta} & \frac{C_{550}}{C_{33}} & 0\\
-\frac{D}{C_{550}}\frac{\kappa_r k_n}{\eta^2} & \frac{D}{C_{550}}\frac{\kappa_r^2}{\eta^2}-\frac{\rho}{\rho_0}\Omega^2 & \frac{\kappa_r}{\eta}\left(\frac{C_{13}}{C_{33}}-1\right) & \frac{k_n}{\eta}\\
\frac{D}{C_{550}}\frac{k_n^2}{\eta^2}-\frac{\rho}{\rho_0}\Omega^2 & -\frac{D}{C_{550}}\frac{\kappa_r k_n}{\eta^2} & -\frac{C_{13}k_n}{C_{33}\eta} & -\frac{2\kappa_r}{\eta}
\end{bmatrix}. \tag{8}$$

where $k_n=n\pi\kappa_s$, $\kappa_s=H/L_0$, $\kappa_r=H/R_0$,$\eta=1+\kappa_r\zeta$, $\Omega=\omega H\sqrt{\rho_0/C_{550}}$ the non-dimensional frequency, and ρ_0 the density value at the inner surface of the arch. Here, Eq. (7) is valid for arbitrary individual layer.

Similarly, the non-dimensional induced variable is

$$X(\zeta) = -\frac{D}{C_{550}}\frac{k_n}{\eta}U + \frac{D}{C_{550}}\frac{\kappa_r}{\eta}W + \frac{C_{13}}{C_{33}}Y. \tag{9}$$

It should be noted that the arch becomes a straight beam when the radius of curvature approaches to infinity, i.e. $R_0 \to \infty$. Under this terminal condition, we have $\kappa_r \to 0$ and $\eta \to 1$, and all terms in Eq. (8) containing κ_r/η vanish. The state equation in Eq. (7) is therefore reduced to Eq. (29) in Chen et al.'s [16] governing the motion of a straight beam.

However, for a circular arch with a finite radius of curvature, Eq. (7) is a differential equation of the state vector $\boldsymbol{\delta}(\zeta)$ about ζ with a variable coefficient matrix $\mathbf{M}$, for which it is rather difficult to seek an analytical solution. To remove the above-mentioned obstacle, the approximate laminate model [17,18] is adopted, in which the individual layer of the arch is further divided into several sub-layers, each being sufficiently thin so that for the individual sub-layer the coordinate ζ can be regarded as constant. With these approximations, Eq. (7) is then reduced to one with constant coefficient matrix for an individual sub-layer. Supposing that each layer of the arch is equally divided into p sub-layers, with the layer thickness $h_{k,j} = h_k/p (j = 1,2, \ldots, p)$. For the jth sub-layer, the ζ-dependent variable η in Eq. (8) is treated as constant by setting $\zeta_{k,j0} = (\zeta_{k,j} - \zeta_{k,j-1})/2$, where $\zeta_{k,j}$ is the radial coordinate of the outer surface of the jth sub-layer in the kth layer. In this circumstance, the state equation for the jth sub-layer is obtained as

$$\frac{\mathrm{d}}{\mathrm{d}\eta}\boldsymbol{\delta}^{(k,j)}(\zeta) = \mathbf{M}_{k,j}(\Omega)\boldsymbol{\delta}^{(k,j)}(\zeta), \tag{10}$$

where $\mathbf{M}_{k,j}$ is now a matrix independent of ζ, the sub- or superscript 'k, j' denotes the jth sub-layer in the kth layer. The general solution is readily sought as

$$\boldsymbol{\delta}^{(k,j)}(\zeta) = \exp\left[(\zeta - \zeta_{k,j-1})\mathbf{M}_{k,j}(\Omega)\right]\boldsymbol{\delta}^{(k,j)}(\zeta_{k,j-1}), \tag{11}$$

for $\zeta_{k,j-1} \leqslant \zeta \leqslant \zeta_{k,j}$ and $j = 1, 2, \ldots, p$. And, hence, there exists

$$\boldsymbol{\delta}_o^{(k,j)} = \mathbf{T}_{k,j}(\Omega)\boldsymbol{\delta}_i^{(k,j)}, \tag{12}$$

where $\mathbf{T}_{k,j}(\Omega) = \exp[h_{k,j}/R_0\mathbf{M}_{k,j}(\Omega)]$ is the transfer matrix of the jth sub-layer, and the subscript 'o' and 'i' represent the values at the outer and inner surfaces, respectively. With the aid of continuity conditions at the interfaces of laminated arches and the artificial interfaces between two adjacent sub-layers, the following relation is obtained:

$$\boldsymbol{\delta}_o^{(p)} = \prod_{j=1}^{p}\mathbf{T}_{m,j}\prod_{j=1}^{p}\mathbf{T}_{m-1,j}\cdots\prod_{j=1}^{p}\mathbf{T}_{2,j}\prod_{j=1}^{p}\mathbf{T}_{1,j}\boldsymbol{\delta}_i^{(1)} = \mathbf{T}(\Omega)\boldsymbol{\delta}_i^{(1)}, \tag{13}$$

where $\mathbf{T}$ is named as the global transfer matrix. For free vibration, the lateral surface of the arch is traction free, that is

$$Y_o = Y_i = 0, \quad \Gamma_o = \Gamma_i = 0. \tag{14}$$

Incorporating the boundary conditions in Eq. (14) into Eq. (13) leads to

$$\begin{bmatrix} T_{31} & T_{32} \\ T_{41} & T_{42} \end{bmatrix}\begin{Bmatrix} U \\ W \end{Bmatrix}_i = \begin{Bmatrix} 0 \\ 0 \end{Bmatrix}_o. \tag{15}$$

A non-trivial solution to Eq. (15) requires the determinant of the coefficient matrix to vanish, that is

$$\begin{vmatrix} T_{31} & T_{32} \\ T_{41} & T_{42} \end{vmatrix} = 0. \tag{16}$$

It should be noted that Eq. (16) is a transcendental equation about Ω^2 and can yields an infinite number of frequency Ω for a given half-wave number n.

3. Numerical examples

3.1. Verifications

To validate the correctness and efficiency of the present formulations, numerical results for simply supported circular arches are compared to those available in literature. Firstly, an isotropic straight beam ($\kappa_r = 0$) is considered as a particular case. Poisson's ratio is $v = 0.167$, and the first ten frequency parameter Ω for beams with different aspect ratios are calculated and listed in Table 1. It is obvious that the present results agree well with that from Timoshenko beam theory [19] for the thin beam, and semi-analytical 2D elasticity solutions [20] for both thin and thick beams.

Secondly, a circular cross-ply laminated arch with the subtended angle $\theta_0 = 1$ rad and the stacking sequence of $90^\circ/0^\circ$ is considered. Each lamina is assumed to have the same thickness and material properties, taken as $E_L = E_T$ or $E_L = 40E_T$, $G_{LT} = G_{TT} = 0.5E_T$, and $v_{LT} = v_{TT} = 0.25$, where the subscripts 'L' and 'T' indicate the directions parallel and perpendicular to the fiber axis. It should be explained that the material properties of $E_L = E_T$ given in Ref. [12] are much like an isotropic material, but the constants E, G and v do not satisfy the relation $E = 2(1+v)G$. Here, this set of material properties are also adopted merely for the purpose of

Table 1
Comparisons of the first ten non-dimensional frequencies $\Omega = \omega H\sqrt{\rho/C_{55}}$ for simply-supported straight beams ($\kappa_r = 0$)

Mode	$H/L = 0.1$			$H/L = 0.3$		
	TBT [19]	Semi. [20]	Present	TBT [19]	Semi. [20]	Present
1	0.042872	0.042878	0.04288	0.34804	0.34845	0.34841
2	0.16442	0.16451	0.16451	1.1097	1.1130	1.11309
3	0.34804	0.34841	0.34841	1.9974	1.4385	1.43823
4	–	0.47990	0.47990	–	2.0069	2.00688
5	0.57578	0.57675	0.57675	2.9154	2.8612	2.86125
6	0.83311	0.83507	0.83507	3.8361	2.9325	2.93250
7		0.95945	0.95945	–	3.8605	3.86057
8	1.1097	1.1131	1.11309	4.7518	4.1579	4.15795
9	1.3988	1.4039	1.40386	5.6608	4.7662	4.76622
10	–	1.4382	1.43823	–	4.7825	4.78192

Table 2
Comparisons of non-dimensional frequencies $\lambda = \omega L_0^2\sqrt{\rho A/E_L I}$ of the first six vibration modes of a two-layered circular arch ($90^\circ/0^\circ$, $\theta_0 = 1$)

E_L/E_T	H/R_0	Results	Mode					
			1	2	3	4	5	6
1	0.1	Present	8.3573	36.205	78.781	113.88	132.19	193.18
		[12]	8.3549	36.153	78.547	113.89	131.57	191.96
	0.2	Present	8.0985	32.282	56.402	64.300	99.899	108.23
		[12]	8.0884	32.124	56.464	63.760	98.806	108.82
	0.25	Present	7.9252	30.184	44.790	57.921	85.533	87.551
		[12]	7.9088	29.969	44.877	57.292	86.376	86.469
40	0.1	Present	2.9961	11.157	21.064	31.650	42.632	53.902
		[12]	3.0816	11.964	23.181	35.118	47.174	59.158
	0.2	Present	2.4085	7.5571	13.181	19.039	24.085	25.022
		[12]	2.5942	8.3991	14.467	20.426	26.275	29.194
	0.25	Present	2.1613	6.4858	11.147	15.962	19.314	20.839
		[12]	2.3666	7.1824	12.015	16.725	21.285	21.352

comparisons and validation of the present formulations. The first six natural frequency parameters $\lambda = \omega L_0^2\sqrt{\rho A/E_L I}$ are calculated and compared to that obtained based on Timoshenko theory [12] in Table 2. Here A and I are the cross-sectional area and the moment of inertia of the arch. Good agreement is again observed for the arches with $E_L = E_T$ and different ratio of H/R_0, thus further validating the efficiency of the present solutions. It is seen that the present results for $E_L = 40E_T$ are much less than those obtained by the Timoshenko theory. Such deviations do not prove the inefficiency of the present 2D results. On the contrary, they imply that the Timoshenko-type model is not necessarily sufficient for arches with high flexibility in shear.

3.2. Effects of geometries and stacking sequences

Effects of the stacking sequences and geometric parameters $\kappa_s(H/L_0)$ and θ_0 (L_0/R_0) on the natural frequencies of cross-ply laminated arches are investigated in this subsection. Shear modulus of the laminates is taken as $G_{LT} = 0.6E_T$ and the other material properties are the same as that in the second validation example in the previous subsection.

Table 3 presents the fundamental frequency parameters $\overline{\omega} = \omega L_0^2\sqrt{\rho/(E_T H^2)}$ of laminated arches with different stacking sequences and the ratio of H/L_0 for the given value of $\theta_0 = 0.2$ rad. Results from the simplified theories for some stacking sequences available in Khdeir and Reddy [10] are also presented for comparison and further validate the efficiency of the present formulations. Compared to the present 2D elasticity solutions, the CAT, SOAT, and the HOAT over-predict the natural frequencies of the considered laminated arches, which is mainly due to the over-accounting of shear rigidity in all these simplified theories. It is observed from Table 3 that the frequency parameter increases but with smaller relative increment as the aspect ratio L_0/H increases. With the increasing of layer numbers for a given geometric definition, the frequency parameter $\overline{\omega}$ increases gradually for antisymmetric laminates, but decrease monotonically for symmetric laminates. The latter is consistent with the physical sense that the bending rigidity of the arch decreases when reducing the partition of lamina with 0^o fiber orientation, while the former indicates that for an antisymmetric laminates, the bending rigidity can be enhanced by increasing layer numbers. This phenomenon is further highlighted by the curves of frequency parameter versus layer number for $L_0 = 5$H in

Table 3
Comparisons of non-dimensional fundamental frequencies $\overline{\omega} = \omega L_0^2\sqrt{\rho/(E_T H^2)}$ of laminated circular arches ($\theta_0 = 0.2$)

L_0/H	Results	Antisymmetric laminates				Symmetric laminate	
		$0°/90°$	$[0°/90°]_2$	$[0°/90°]_5$	$0°/90°/0°$	$[0°/90°]_2/0°$	$[0°/90°]_4/0°$
5	Present	5.7140	7.3546	8.0222	9.1376	8.9820	8.7429
	HOAT[a]	6.156			9.190		
	SOAT[a]	5.893			9.798		
	CAT[a]	7.174			17.387		
10	Present	6.7825	9.9334	10.7908	13.5232	12.8539	12.1567
	HOAT	6.961	10.212	10.880	13.586		
	SOAT	6.863	–	–	14.121		
	CAT	7.288	11.712	12.667	17.597		
50	Present	7.2644	11.6130	12.5660	17.3555	15.8292	14.5756
	HOAT	7.294			17.427		
	SOAT	7.290			17.472		
	CAT	7.310			17.666		
100	Present	7.2757	11.6760	12.6351	17.5360	15.9595	14.6772
	HOAT	7.303			17.608		
	SOAT	7.302			17.619		
	CAT	7.307			17.668		

[a]Results are obtainable in Khdeir and Reddy [10].

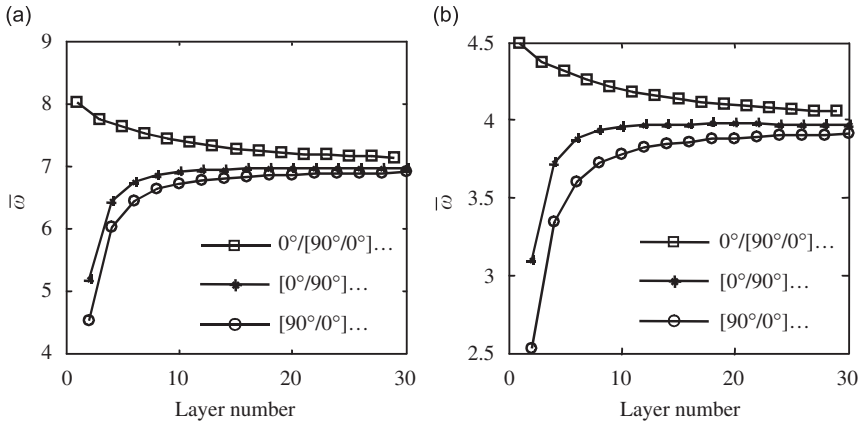

Fig. 2. Variations of fundamental frequency parameter $\overline{\omega} = \omega L_0^2\sqrt{\rho/(E_T H^2)}$ versus the layer number of circular arches with different subtended angle ($L = 5H$).

Fig. 2, with indication that the natural frequency of antisymmetric arches are more sensitive to the increasing of layer number than that of symmetric laminates. Presented in Fig. 2 are also the comparisons of the curves for two types of antisymmetric laminates, one with the 0° lamina at the inner surface (asterisk marker) and the other with 90° lamina at the inner surface (circle marker). It is seen that the fundamental frequency of the former type of antisymmetric arch is higher than the latter, but the variation of frequency against the layer number is quite similar to each other.

Fig. 3 shows the variations of the fundamental frequency parameters $\overline{\omega}$ versus the increasing of the subtended angle θ_0 (rad) for circular arches with different thickness-to-length ratios and stacking sequences. In the figures, the abscissa represents the subtended angle θ_0 which varies so that $0 \leqslant \theta_0 \leqslant 3$, and the ordinate indicates the frequency parameter $\overline{\omega}$ for various θ_0. It is seen from the figures that the $\overline{\omega} - \theta_0$ curves ascend in an approximately linear manner when the subtended angles of all considered arches decrease from 3 to 1 rad. However, when the subtended angles θ_0 decrease continuously to 0 rad (straight beams), the curves deviate downward away from the linear trend when $\theta_0 > 1$, that is, the increasing of frequencies slow down when the arches approaches increasingly toward the straight beams. It is also observed that the slopes of the curves for $L_0/H = 20$ are largest while those for $L_0/H = 5$ are the smallest. This implies that the thinner the arches, the more sensitive of the fundamental frequencies are to the variations of the subtended angles. Deep comparisons between Figs. 3a and c (or Figs. 3b and d) show that, for antisymmetric stacking sequences, the fundamental frequencies of the arches with 0° laminate closer to the inner surface are slightly higher than those of the arches with 0° laminate closer to outer surface. In addition, the nonlinearity of the curves between $0 \leqslant \theta_0 \leqslant 1$ of the former arches is more obvious than that of the later arches. Finally, for a same aspect ratio, the fundamental frequencies of the arches with symmetric stacking schemes (Figs. 3e and f) are greater than those of the antisymmetric laminated arches (Figs. 3a–d). Furthermore, the former arches attain a more sensitivity to the changes of the subtended angles than the latter do.

4. Conclusions

Exact two-dimensional elasticity solutions are derived for the in-plane vibration of simply supported laminated composite circular arches using the state space method. The present state equation is also applicable to straight beams when setting the radius of curvature to infinite, and was validated by comparing the numerical results to those obtained in literature. The present method is validated by comparing numerical results with those obtained for straight, isotropic curved, or laminated curved beams based on other shear deformable theories. The present 2D solution does not adopt any assumptions about the distribution of displacements of strains along the thickness direction, and hence, it is applicable for both slender and thick circular arches.

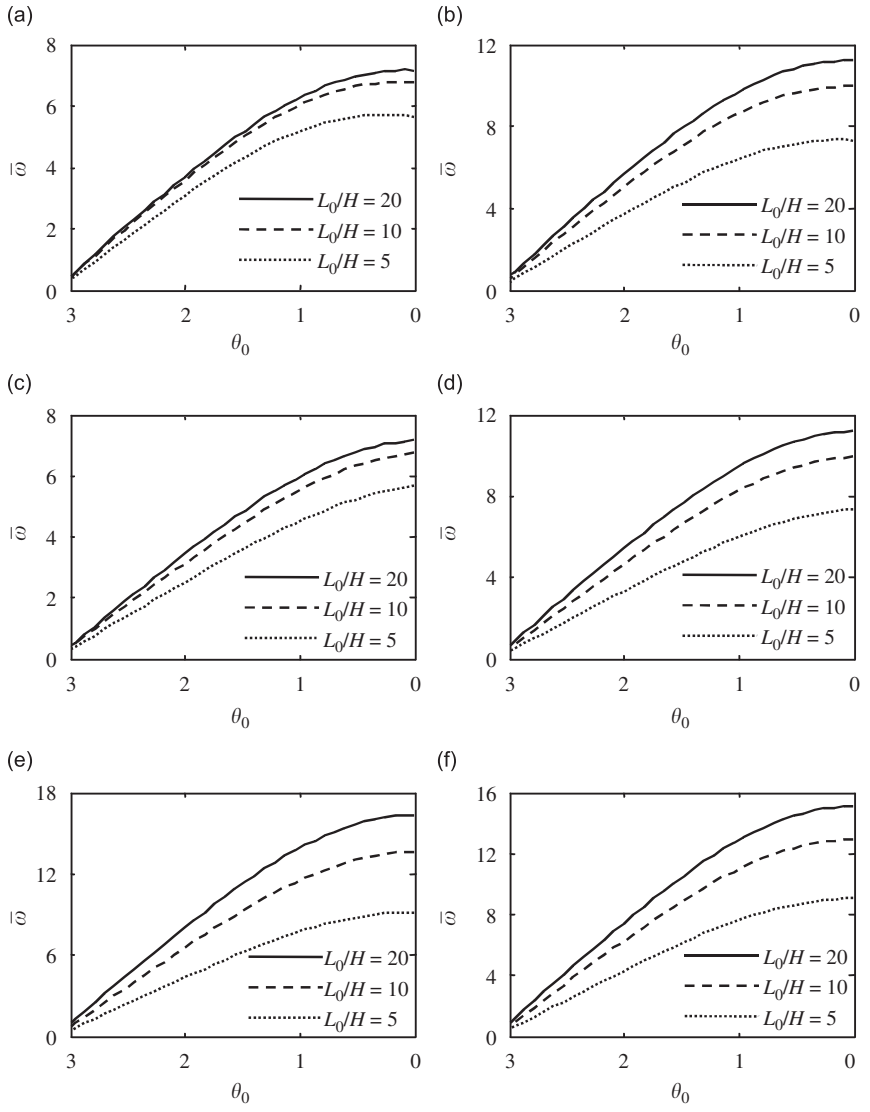

Fig. 3. Variations of fundamental frequency parameters $\overline{\omega} = \omega L_0^2\sqrt{\rho/(E_T H^2)}$ versus the subtended angle θ_0 (rad) for circular arches with different length and stacking sequences.

Effect of thickness-to-length ratio, subtended angle and stacking sequences on in-plane natural frequencies of circular arches are investigated. It is interesting that antisymmetric laminates with exchanged spatial location of 0° and 90° lamina behave different versus the variation of subtended angle. Numerical results presented in this paper are expected to serve as benchmarks for other numerical simulations and simplified theories for circular arches.

Acknowledgments

This work was supported by the National Natural Science Foundation of China (Nos. 10702061 and 10432030). It was also partly supported by the China Postdoctoral Science Foundation (Nos. 20060401071 and 20070421201).

References

[1] P.A.A. Laura, M.J. Maurizi, Recent research on vibrations of arch-type structures, *Shock and Vibration Digest* 19 (1987) 6–9.
[2] P. Chidamparam, A.W. Leissa, Vibration of planar curved beams, rings, and arches, *Applied Mechanics Reviews* 46 (1993) 467–483.
[3] E. Tüfekçi, A. Arpaci, Exact solution of in-plane vibrations of circular arches with account taken of axial extension, transverse shear and rotatory inertia, *Journal of Sound and Vibration* 209 (1998) 845–856.
[4] B. Kang, C.H. Riedel, C.A. Tan, Free vibration analysis of planar curved beams by wave propagation, *Journal of Sound and Vibration* 260 (2003) 19–44.
[5] E. Viola, E. Artioli, M. Dilena, Analytical and differential quadrature results for vibration analysis of damaged circular arches, *Journal of Sound and Vibration* 288 (2005) 887–906.
[6] E. Tufekci, O. Ozdemirci, Exact solution of free in-plane vibration of a stepped circular arch, *Journal of Sound and Vibration* 295 (2006) 725–738.
[7] E. Viola, M. Dilena, F. Tornabene, Analytical and numerical results for vibration analysis of multi-stepped and multi-damaged circular arches, *Journal of Sound and Vibration* 299 (2007) 143–163.
[8] A. Bhimaraddi, A.J. Carr, P.J. Moss, Generalized finite element analysis of laminated curved beams with constant curvature, *Computers and Structures* 31 (1989) 309–317.
[9] M.S. Qatu, In-plane vibration of slightly curved laminated composite beams, *Journal of Sound and Vibration* 159 (1992) 327–338.
[10] A.A. Khdeir, J.N. Reddy, Free and forced vibration of cross-ply laminated composite shallow arches, *International Journal of Solids and Structures* 34 (1997) 1217–1234.
[11] V. Yildirim, Rotary inertia, axial and shear deformation effects on the in-plane natural frequencies of symmetric cross-ply laminated circular arches, *Journal of Sound and Vibration* 224 (1999) 575–589.
[12] Y.P. Tseng, C.S. Huang, M.S. Kao, In-plane vibration of laminated curved beams with variable curvature by dynamic stiffness analysis, *Composite Structures* 50 (2000) 103–114.
[13] H. Matsunaga, Free vibration and stability of laminated composite circular arches subjected to initial axial stress, *Journal of Sound and Vibration* 271 (2004) 651–670.
[14] L.Y. Bahar, A sate space approach to elasticity, *Journal of the Franklin Institute* 299 (1975) 33–41.
[15] J.R. Vinson, R.L. Sierakowski, *The Behavior of Structures Composed of Composite Materials*, second ed., Kluwer, London, 2002.
[16] W.Q. Chen, C.F. Lv, Z.G. Bian, Elasticity solution for free vibration of laminated beams, *Composite Structures* 62 (2003) 75–82.
[17] W.Q. Chen, H.J. Ding, Bending of functionally graded piezoelectric rectangular plates, *Acta Mechanica Solida Sinica* 13 (2000) 312–319.
[18] W.Q. Chen, L.Z. Wang, Y. Lu, Free vibrations of functionally graded piezoceramic hollow spheres with radial polarization, *Journal of Sound and Vibration* 251 (2002) 103–114.
[19] H.C. Hu, *Variational Principles of Theory of Elasticity with Applications*, Gordon and Breach, New York, 1984.
[20] W.Q. Chen, C.F. Lu, Z.G. Bian, A semi-analytical method for free vibration of straight orthotropic beams with rectangular cross-sections, *Mechanics Research Communications* 31 (2004) 725–734.